Research Article

Parallactic delay for geodetic VLBI and non-orthogonality of the fundamental axes

Oleg Titov[1] and Angelina Osetrova[2]

[1]Geoscience Australia, Canberra, Australia and [2]Saint-Petersburg State University, Saint-Petersburg, Russia

Abstract

The Gaia optical astrometric mission has measured the precise positions of millions of objects in the sky, including extragalactic sources also observed by Very Long Baseline Interferometry (VLBI). In the recent Gaia EDR3 release, an effect of negative parallax with a magnitude of approximately $-17\,\mu$as was reported, presumably due to technical reasons related to the relativistic delay model. A recent analysis of a 30-yr set of geodetic VLBI data (1993–2023) revealed a similar negative parallax with an amplitude of $-15.8 \pm 0.5\,\mu$as. Since both astrometric techniques, optical and radio, provide consistent estimates of this negative parallax, it is necessary to investigate the potential origin of this effect.

We developed the extended group relativistic delay model to incorporate the additional parallactic effect for radio sources at distances less than 1 Mpc and found that the apparent annual signal might appear due the non-orthogonality of the fundamental axes, which are defined by the positions of the reference radio sources themselves. Unlike the conventional parallactic ellipse, the apparent annual effect in this case appears as a circular motion for all objects independently of their ecliptic latitude. The measured amplitude of this circular effect is within a range of 10–15 μas that is consistent with the ICRF3 stability of the fundamental axis. This annual circular effect could also arise if a Gödel-type cosmological metric were applied, suggesting that, in the future, this phenomenon could be used to indicate global cosmic rotation.

Keywords: Astrometry; reference systems; methods: data analysis; cosmology: theory

1. Introduction

The Very Long Baseline Interferometry (VLBI) technique measures the time difference (time delay) between the arrivals of a radio signal from a distant source at two radio telescopes separated by a long baseline (Schuh & Behrend 2012). This time delay is calculated by correlating the signals recorded at both stations, using either hardware or software correlators. By observing many radio sources over extended periods, highly accurate position estimates for these sources can be achieved.

Two previous fundamental catalogues of reference radio sources, ICRF1 and ICRF2, were released in 1995 (Ma et al. 1998) and 2009 (Fey et al. 2015), respectively. The current International Celestial Reference Frame (ICRF3) is based on the positions of 4 536 radio sources observed between 1979 and 2018, of which 303 are 'defining' sources that define the fundamental axes with an uncertainty of 30 μas (Charlot et al. 2020). The formal errors of individual radio source positions vary widely due to the uneven number of observations, ranging from 6 μas to a few mas.

The relativistic model for the VLBI group delay, as published in the IERS Conventions 2010 (Petit & Luzum 2010), accounts for the relativistic effects of both special and general relativity with a precision of 1 ps. However, this model does not include the parallactic delay, as almost all radio sources observed by geodetic VLBI are located beyond 1 Mpc. A few galactic radio stars are treated similarly to extragalactic objects (Lunz et al. 2023). Recently, Soffel, Kopeikin, & Han (2017) extended the conventional model to include closer objects, but this advanced model has not yet been adopted by the IERS Conventions.

In the recent Gaia EDR3 release, a negative annual parallax with an amplitude of approximately $-17\,\mu$as was reported for extragalactic active galactic nuclei (AGNs) observed in optical wavelengths (Lindegren et al. 2021). The authors suggested that this effect might be due to the design of the Gaia telescope, which introduces calibration challenges related to the angle between its two mirrors, thus leading to the zero parallax point offset (e.g. Groenewegen 2021). Accurate parallax measurements are crucial for various applications (Butkevich et al. 2017), making additional verification of this estimate essential.

Since nearly all radio sources observed by geodetic VLBI are at extragalactic distances, their parallax has long been considered to be negligible and has therefore never been estimated. However, Titov et al. (2024) recently identified a similar negative annual parallax of $-15.8 \pm 0.5\,\mu$as, based on 30 yr of geodetic VLBI observations from 1993 to 2023. New CRF solution (aus2024a.crf[a]) enlarges the number of group delays to 15 millions, that is, approximately on 2 millions more than used for ICRF3 catalogue (Charlot et al. 2020). A new catalogue comprises coordinates of 5 428 radio sources with three or more observations, that is, almost 1 000 more than in ICRF3. The formal errors of the most observed radio sources is about 2–3 μas. Such progress encourages

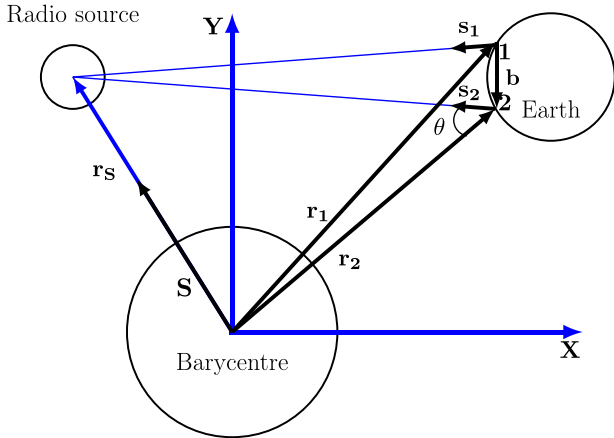[a]https://cddis.nasa.gov/archive/vlbi/ivsproducts/crf/.

Figure 1. Mutual positions of two radio telescopes on Earth and a radio source in the barycentric reference frame.

the investigation of a hidden systematic that could be missed in the previous solutions.

It remains unclear whether the optical and radio instruments are detecting the same phenomenon or if this is merely a numerical coincidence between two independent effects.

To address this ambiguity, we develop an analytical VLBI delay model that includes parallax and explore possible origins for an annual signal that is independent of the distance to the observed objects.

2. Parallactic Delay

For all extragalactic radio sources at a distance R greater than 1 Mpc, the annual parallax is less than 1 μas, and the corresponding parallactic delay is negligible. Consequently, the equation for the parallactic delay has not been formulated until 2017 (Soffel et al. 2017). In this work, we develop the equation for the parallactic delay in a form that is convenient for implementation in coding and consider alternative of the annual signal appearance apart from the classical astrometric explanation.

The standard approach involves considering the difference between the barycentric coordinates of two radio telescopes, $r_1(t_1)$ and $r_2(t_2)$, to represent the difference in time propagation τ as follows (Fig. 1):

$$\tau = t_2 - t_1 = t_{2S} + t_{2E} - (t_{1S} + t_{1E}) \tag{1}$$

where

$$\tau = \frac{r_S s_2}{c} - \frac{r_2 S}{c} - \left(\frac{r_S s_1}{c} - \frac{r_1 S}{c}\right) =$$
$$= \frac{r_S s_2}{c} - \frac{r_S s_1}{c} - \left(\frac{r_2 S}{c} - \frac{r_1 S}{c}\right) = \tag{2}$$
$$= \tau_S + \tau_E$$

The first term in equation (2) represents the time delay propagation from an extragalactic radio source to the Solar System barycenter, while the second term accounts for the local Solar System effects. If we ignore the parallactic effect, then $\tau_S = 0$, and the total delay (1) is reduced to the geometric delay τ_E in its simplest form. Denoting the vector baseline as $r_2 - r_1 = b$,

$$\tau = \tau_E = -\frac{(r_2 - r_1)S}{c} = -\frac{(bS)}{c} \tag{3}$$

Equation (3) presents the geometric delay in its simplest form. In the full form, it expands to the relativistic delay including all effects of special relativity and the retarded baseline correction due to the geocentric motion of the both radio telescopes. It is fully consistent to the official IERS Conventions 2010 model (Petit & Luzum 2010); therefore, any additional terms developed in the paper may be simply added to the conventional equation. Typically, only the expanded version of equation (3) is used for modelling geodetic VLBI observations of extragalactic objects. However, if we wish to account for the parallactic effect in the time delay, the first term τ_S in equation (2) must be elaborated. Throughout the manuscript, all additional terms will be developed in the same way as the conventional equations in previous papers (Titov & Girdiuk 2015; Titov, Melnikov, & Lopez 2020).

In the general case, the unit direction vectors from each radio telescope to an extragalactic object differ (i.e. $s_1 \neq s_2$), and the equation for s_i (where $i = 1, 2$) is given by:

$$s_i = \frac{r_{is}}{|r_{is}|} = \frac{r_S - r_i}{\sqrt{r_S^2 - 2(r_S r_i) + r_i^2}} \tag{4}$$

and, as for an extragalactic radio source $r_S \gg r_i$

$$s_i = \frac{r_S - r_i}{|r_S|\sqrt{1 - \frac{2(r_S r_i)}{r_S^2} + \frac{r_i^2}{r_S^2}}} \tag{5}$$

Then, using the well-known expansion:

$$\frac{1}{\sqrt{1+x}} \approx 1 - \frac{x}{2} + \frac{3x^2}{8} - \frac{5x^3}{16} + \ldots \tag{6}$$

one could convert (5) as follows:

$$s_i \approx \frac{r_S - r_i}{|r_S|}\left(1 - \frac{1}{2}\left(\frac{r_i^2}{r_S^2} - \frac{2(r_i r_S)}{r_S^2}\right) + \right.$$
$$\left. + \frac{3}{8}\left(\frac{r_i^2}{r_S^2} - \frac{2(r_i r_S)}{r_S^2}\right)^2\right) \tag{7}$$

By defining $S = \frac{r_S}{|r_S|}$ and truncating terms of the order $O\left(\frac{r_i^3}{r_S^3}\right)$ and higher one can obtain:

$$s_i \approx S - \frac{S}{2}\frac{r_i^2}{r_S^2} + \frac{(r_i S)S - r_i}{|r_S|} + \frac{3(r_i S)^2 S}{2|r_S|^2} - \frac{(r_i S)r_i}{|r_S|^2} =$$
$$= S + \frac{(r_i S)S - r_i}{|r_S|} - \tag{8}$$
$$- \frac{1}{|r_S|^2}\left((r_i S)r_i + \frac{S r_i^2}{2} - \frac{3(r_i S)^2 S}{2}\right)$$

Therefore, for $(r_S s_i)$

$$(r_S s_i) \approx (r_S S) + \frac{(r_i S)(r_S S) - (r_S r_i)}{|r_S|} -$$
$$- \frac{1}{|r_S|^2}\left((r_i S)(r_S r_i) + \frac{(r_S S)r_i^2}{2} - \frac{3(r_i S)^2(r_S S)}{2}\right) \tag{9}$$

As $(r_S S) = |r_S|$, the second term in (9) disappears, and

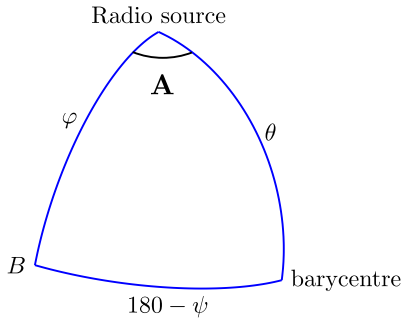$$(r_S s_i) \approx |r_S| + \frac{1}{2|r_S|}\left((r_i S)^2 - r_i^2\right) \tag{10}$$

Figure 2. Spherical triangle formed by three vectors, s_2, b, and r_2, with respect to the Earth's geocentre. Point B lies on the celestial sphere along the extension of vector b.

Therefore, for τ_S in (2)

$$\tau_S = \frac{(r_S s_2) - (r_S s_1)}{c} =$$
$$= \frac{1}{2c|r_S|}\left((r_2 S)^2 - r_2^2\right) - \frac{1}{2c|r_S|}\left((r_1 S)^2 - r_1^2\right) \quad (11)$$

and, denoting $|r_S| = r_S$

$$\tau_S = \frac{(r_2 S)^2 - (r_1 S)^2 - r_2^2 + r_1^2}{2c r_S} \quad (12)$$

Equation (12) provides a precise model for the parallactic delay; however, the parallax (π) is not explicitly presented here. To obtain the classical form, the baseline vector must be introduced using the equation $b = r_2 - r_1$.

$$\tau_S = \frac{(r_2 S)^2 - ((r_2 - b)S)^2 - r_2^2 + (r_2 - b)^2}{2c r_S} =$$
$$= \frac{2(r_2 S)(bS) - (bS)^2 - 2(br_2) + |b|^2}{2c r_S} \quad (13)$$

Now, consider the spherical triangle (Fig. 2) where θ is the angle between the vectors s_2 and $-r_2$ (in this context, θ is the elongation angle between the directions from station 2 to the barycenter and the radio source), φ is the angle between the vectors s_2 and b, ψ is the angle between b and r_2, and angle A links all the angles together through the spherical trigonometry equation:

$$\cos\psi = -\cos\varphi\cos\theta - \sin\theta\sin\varphi\cos A \quad (14)$$

As an extragalactic radio source is on cosmological distance, we consider that $r_2 \ll r_S$ and $(r_2 S) \approx (r_2 s_2) \approx (r_2 s_1) = -r_2\cos\theta$, therefore, from equation (13)

$$\tau_S = \frac{-2br_2\cos\varphi\cos\theta - 2br_2\cos\psi + b^2(1 - \cos^2\varphi)}{2c r_S} \quad (15)$$

and applying (14)

$$\tau_S = \frac{r_2\sin\theta}{r_S}\frac{b}{c}\sin\varphi\cos A + \frac{b}{c}\frac{b\sin^2\varphi}{2r_S} \quad (16)$$

Now the astrometric parallax appears in the classical form $\pi = \frac{r_2}{r_S}$ in the first term of (16). Denoting $\pi' = \frac{b}{2r_S}$ as an 'additional' baseline parallactic displacement, if the baseline is long enough to detect the corresponding effect, one could present the final equation as follows:

$$\tau_S = \pi\frac{b}{c}\sin\theta\sin\varphi\cos A + \pi'\frac{b}{c}\sin^2\varphi \quad (17)$$

Keeping only the first term in (17), the equation for $\Delta\theta$ could be formulated in terms of the vector form

$$\tau_S = \frac{(r_2 s_2)(bs_2) - (br_2)}{c r_S} =$$
$$= \frac{|r_2|}{r_S}\frac{N(s_2(bs_2) - b)}{c} = \quad (18)$$
$$= \pi\frac{N(s_2(bs_2) - b)}{c}$$

where $N = \frac{r_2}{|r_2|}$ is the unit vector directed from the barycenter towards station 2. It should be noted that equation (17) corresponds to the equation from the paper by Soffel et al. (2017) but is easier for coding.

In classical astrometric observations of parallax, an Earth-based observer measures the relative displacement of a foreground object with respect to background reference objects. For a positive meaning of the parallax, the apparent elongation angle, $\theta' = \theta + \Delta\theta$, is smaller than the elongation angle corresponding to the unperturbed position. This results in the observed object appearing shifted towards the Sun ($\Delta\theta \leq 0$) in a case of positive parallax, that is, $\pi = -\Delta\theta$,.

A hypothetical parallactic displacement in the opposite direction, where the object appears to move away from the Sun, would result in an increase in the apparent elongation angle ($\Delta\theta \geq 0$). In the classical interpretation, such a shift would imply that the foreground object is, paradoxically, further from the Sun than the background reference sources. This corresponds to a positive sign of the elongation angle change, and, inevitably, to a negative value of the annual parallax.

In classical astrometry, this scenario is unrealistic, as it suggests an inversion of the standard spatial relationships. Thus, any parallax of this nature should be referred to as 'negative parallax', irrespective of its physical origin. Possible reasons for the effect's origin is discussed in two next sections.

3. Violation of Orthogonality of Fundamental Axes

The orientation of the fundamental axes is defined by the positions of so-called 'defining' radio sources. However, all of these radio sources are known to be AGNs, which often exhibit extended and variable structures. Even when the structure is stable, the phase response of an interferometer depends on the baseline length and the complexity of the structure. In the worst-case scenario, the position of the same extended radio source, when measured by short and long VLBI baselines, may differ by several milliarcseconds (mas) (Charlot et al. 2020).

Additionally, systematic effects such as secular aberration drift (SAD), with an amplitude of 5–6 μas/yr (as discussed by Titov, Lambert, & Gontier 2011, and MacMillan et al. 2019), caused by the galactocentric acceleration of the Solar System, also impact the orientation of the fundamental axes. For instance, an uncertainty in the SAD amplitude of 1 μas/yr could result in a displacement of the fundamental axes by 30 μas over a 30-yr period of observations (Fey et al. 2015; Charlot et al. 2020). Consequently, a deviation of the axes from orthogonality by as much as 10–15 μas is not out of the question.

Now, consider the scenario where the X and Y axes are not perfectly orthogonal (Fig. 3). The additional term to describe the
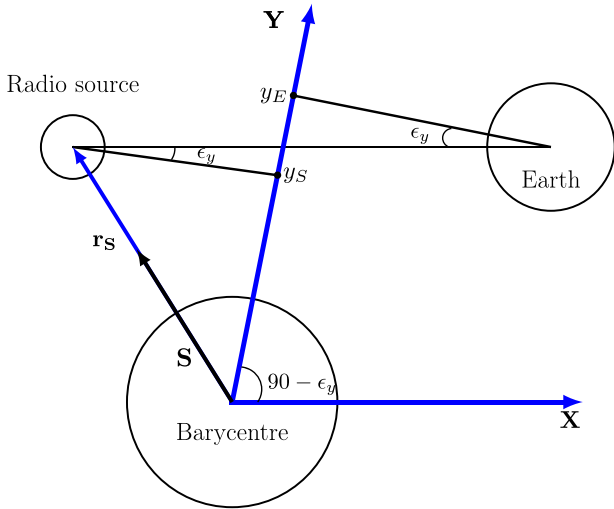
Figure 3. Mutual position of the Earth and a radio source in the barycentric reference frame in a case if the axes X and Y are not orthogonal. The angle between X and Y is $(90 - \epsilon_y)$ degrees. This leads that the projecton of the signal travel path on the axes Y $y_E - y_S$ is non-zero.

propagation of light from a radio source to the Earth along the Y-axis over the time interval dt can be expressed as follows:

$$cdt = dx + \epsilon_y dy \tag{19}$$

where ϵ_y is a deviation of the angle between X and Y from 90 degrees, $\epsilon_y \ll 1$

After integration of the second term in (19)

$$c\tau_y = \epsilon_y (y_2 - y_1) \tag{20}$$

Since we are using a barycentric coordinate system, the projection of the signal travel path from the radio source to stations 1 and 2 onto the X and Y axes must be considered. The projection onto the X-axis was already presented in the previous section as the difference in dot products: $(\boldsymbol{r_S s_2}) - (\boldsymbol{r_S s_1}) = x_2 - x_1$ as shown in equation (11).

In the case where the X and Y axes are orthogonal, the difference $y_2 - y_1$ should ideally be zero. However, if $\epsilon_y \neq 0$ (i.e. there is a small deviation), the corresponding projection along the Y-axis is given by: $y_i^2 = \boldsymbol{r_S}^2 - (\boldsymbol{r_S s_i})^2$.

From equation (10), we have $(\boldsymbol{r_S s_i})^2 \approx r_S^2 + ((\boldsymbol{r_i S})^2 - r_i^2)$. Therefore, the time delay along the Y-axis, as described in equation (20), can be derived accordingly:

$$c\tau_y = \epsilon_y (\sqrt{r_S^2 - (\boldsymbol{r_S s_2})^2} - \sqrt{r_S^2 - (\boldsymbol{r_S s_1})^2}) \approx$$
$$\approx \epsilon_y (\sqrt{\boldsymbol{r_2}^2 - (\boldsymbol{r_2 S})^2} - \sqrt{\boldsymbol{r_1}^2 - (\boldsymbol{r_1 S})^2}) \tag{21}$$

Equation (21) mirrors the form of (12) from the previous section.

$$\tau_y = \epsilon_y \frac{\sqrt{\boldsymbol{r_2}^2 - (\boldsymbol{r_2 S})^2} - \sqrt{\boldsymbol{r_1}^2 - (\boldsymbol{r_1 S})^2}}{c} \tag{22}$$

By substituting $\boldsymbol{r_1} = \boldsymbol{r_2} - \boldsymbol{b}$ into (22):

$$\tau_y = \frac{\epsilon_y}{c}\sqrt{\boldsymbol{r_2}^2 - (\boldsymbol{r_2 S})^2} - \frac{\epsilon_y}{c}\sqrt{(\boldsymbol{r_2} - \boldsymbol{b})^2 - ((\boldsymbol{r_2} - \boldsymbol{b})\boldsymbol{S})^2} \tag{23}$$

Defining $\boldsymbol{N} = \frac{\boldsymbol{r_2}}{|\boldsymbol{r_2}|}$

$$\tau_y = \frac{\epsilon_y |\boldsymbol{r_2}|}{c}\sqrt{1 - (\boldsymbol{NS})^2} - \frac{\epsilon_y |\boldsymbol{r_2}|}{c} \cdot$$
$$\cdot \sqrt{1 - (\boldsymbol{NS})^2 - 2\frac{(\boldsymbol{Nb}) - (\boldsymbol{NS})(\boldsymbol{bS})}{|\boldsymbol{r_2}|} + \frac{\boldsymbol{b}^2 - (\boldsymbol{bS})^2}{|\boldsymbol{r_2}|^2}} \tag{24}$$

After extracting $\sqrt{1 - (\boldsymbol{NS})^2}$ from the second term and performing Taylor series expansion (6) up to the second term, we obtain the following equation.

$$\tau_y = \frac{\epsilon_y}{c} \cdot \left(\frac{(\boldsymbol{Nb}) - (\boldsymbol{NS})(\boldsymbol{bS})}{\sqrt{(1 - (\boldsymbol{NS})^2)}} - \frac{\boldsymbol{b}^2 - (\boldsymbol{bS})^2}{2|\boldsymbol{r_2}|\sqrt{(1 - (\boldsymbol{NS})^2)}} \right) \tag{25}$$

As $1 - (\boldsymbol{NS})^2 = \sin^2 \theta$, substituting this into equation (25):

$$\tau_y = \frac{\epsilon_y}{c} \cdot \left(\frac{(\boldsymbol{Nb}) - (\boldsymbol{NS})(\boldsymbol{bS})}{\sin \theta} - \frac{\boldsymbol{b}^2 - (\boldsymbol{bS})^2}{2|\boldsymbol{r_2}|\sin \theta} \right) =$$
$$= \frac{\epsilon_y}{c \sin \theta} \left((\boldsymbol{Nb}) - (\boldsymbol{NS})(\boldsymbol{bS}) - \frac{\boldsymbol{b}^2 - (\boldsymbol{bS})^2}{2|\boldsymbol{r_2}|} \right) \tag{26}$$

Applying the spherical triangle equations and (14) we proceed:

$$\tau_y = \frac{\epsilon_y}{c \sin \theta} \left(-b \sin \theta \sin \varphi \cos A - \frac{\boldsymbol{b}^2 \sin^2 \varphi}{2|\boldsymbol{r_2}|} \right) =$$
$$= -\epsilon_y \frac{b}{c} \sin \varphi \cos A - \epsilon_y \frac{\boldsymbol{b}^2 \sin^2 \varphi}{2c|\boldsymbol{r_2}| \sin \theta} \tag{27}$$

After truncation of the small term in (27)

$$\tau_y = -\epsilon_y \frac{b}{c} \sin \varphi \cos A \tag{28}$$

Consequently, equation (27) bears resemblance to the parallax effect equation from the first term of (17), but with two significant differences: it is independent of the distance and lacks the factor $\sin \theta$ in numerator. In other words, this apparent displacement affects all objects uniformly, regardless of their distance, and manifests as a circular motion with an amplitude of ϵ_y, as opposed to the traditional parallactic ellipse. This effect reflects the non-orthogonality of the fundamental X and Y axes. It is evident that the observed effect can be either positive or negative, depending on the sign of the small parameter ϵ_y.

4. Implication of Cosmological Metrics

Now, let us consider the stationary cosmological metric of the Gödel type, as discussed in previous works (Obukhov 1992; Korotky & Obukhov 1996; Korotky, Masár, & Obukhov 2020):

$$dS^2 = c^2 dt^2 - dx^2 - 2\sqrt{\sigma} e^{mx} cdtdy - ke^{2mx} dy^2 - dz^2 \tag{29}$$

Here, m, k, and σ are constant parameters. In the classical Gödel metric (Gödel 1949), with $m = 1$, $\sigma = 1$, and $k = -\frac{1}{2}$, closed time-like curves exist, leading to causality violations. However, an extended version of the metric avoids this issue if $k > 0$. The global rotation is directed along the Z-axis, with the magnitude of the rotation, ω, determined by these parameters in this form:

$$\omega = \frac{m}{2}\sqrt{\frac{\sigma}{\sigma + k}} \tag{30}$$

The vorticity vanishes when either m or σ is zero. Although further generalisations of the metric are possible (Obukhov 1992), such cases are not essential for our current discussion.

For simplicity, let us consider the metric in the plane perpendicular to the rotation axis Z.

$$dS^2 = c^2 dt^2 - 2\sqrt{\sigma}\, e^{mx} c\, dt\, dy - k e^{2mx} dy^2 - dx^2 - dz^2 \quad (31)$$

For the equation of the elementary interval $dS^2 = 0$ one could find a solution for the time interval dt Solving the equation for the elementary interval $dS^2 = 0$, we can derive an expression for the time interval dt, assuming that $y'_x = \frac{dy}{dx} \ll 1$ and $z'_x = \frac{dz}{dx} \ll 1$.

$$
\begin{aligned}
cdt &= \sqrt{\sigma}\, e^{mx} dy \pm \\
&\pm \sqrt{\sigma e^{2mx} dy^2 + k e^{2mx} dy^2 + dx^2 + dz^2} = \\
&= \sqrt{\sigma}\, e^{mx} dy \pm \sqrt{dx^2\left(1 + (\sigma + k)e^{2mx}\frac{dy^2}{dx^2} + \frac{dz^2}{dx^2}\right)} = \\
&= \sqrt{\sigma}\, e^{mx} dy \pm dx\sqrt{1 + (\sigma + k)e^{2mx}y'^2_x + z'^2_x} \approx \\
&\approx \sqrt{\sigma}\, e^{mx} dy \pm dx\left(1 + \frac{(\sigma + k)e^{2mx}y'^2_x}{2} + \frac{z'^2_x}{2}\right)
\end{aligned}
\quad (32)
$$

In equation (32), we select the positive sign:

$$cdt = \left(1 + \frac{(\sigma + k)e^{2mx}y'^2_x}{2} + \frac{z'^2_x}{2}\right)dx + \sqrt{\sigma}\, e^{mx} dy \quad (33)$$

The first term in (33) corresponds to the standard geometric VLBI delay. Thus, variations in the Earth's scale factor (mean radius) could be detectable, provided that y'_x and $z'_x \neq 0$. This implies that the possible global rotation of the Universe could, in principle, be detected using standard VLBI techniques, were m large enough. Even if y'_x and $z'_x = 0$ (i.e. all three spatial axes are orthogonal), an additional term remains, which can be expressed in the form of (19) with the parameter ϵ_y:

$$\epsilon_y = \sqrt{\sigma}\, e^{mx} \quad (34)$$

If we set $m = 0$ and $e^{mx} = 1$, then

$$\epsilon_y = \sqrt{\sigma}, \quad (35)$$

The additional effect is still non-zero in equation (35), even if the global rotation (30) vanishes ($\omega = m = 0$). A non-zero σ in the metric (29) is sufficient to produce a constant annual effect observable across the entire sky, independent of distance. If both parameters σ and m are non-zero, the global rotation, if it exists, would contribute to the basic effect.

5. Discussion and Conclusion

Recent optical and VLBI observations have detected a negative parallax, drawing widespread interest due to the contentious nature of its origin. The classical parallactic delay, which includes the astrometric annual parallax, was not considered in this case for a straightforward reason: all extragalactic radio sources observed by geodetic VLBI are far too distant for an Earth-based observer to measure classical parallax, and the number of sufficiently strong galactic radio stars is limited. However, the analytical expression given in equation (17) remains useful, as it explicitly illustrates the dependence on the elongation angle, θ.

Interestingly, we discovered that a similar analytical dependence could arise from a more mundane cause, such as a violation of the orthogonality of the fundamental axes. In this scenario, an annual effect (though not strictly parallactic in the classical sense but rather its 'circular' analogue) if detected would be independent of the object's distance. Therefore, this 'quasi-parallax' effect is expected to manifest in extragalactic objects, given that the fundamental axes are determined by the coordinates of defining radio sources. Currently, there is no reliable method for independently verifying the orthogonality of these axes. Therefore, the proposed technique could be used as a handy tool to control the direct angle between the fundamental axes with sufficient accuracy. It is known that the astrometric positional stability is compromised by variations in the intrinsic structure of radio sources, with amplitudes reaching several milliarcseconds due to high-energy processes occurring in the cores of AGNs. As such, continuous monitoring of this combined instability in the fundamental axes is essential.

Furthermore, non-standard cosmological metrics, such as the classical Gödel solution or a Bianchi-type III model (29), might also produce an apparent annual effect. However, in these cases, the amplitude would depend on different model parameters. If the measured amplitude of the annual effect remains stable over an extended period, it could provide a basis for speculating on the estimation of specific parameters within these metrics (e.g. a global rotation of the Universe). Nonetheless, such speculation remains beyond the scope of this manuscript.

References

Butkevich, A., Klioner, S., Lindegren, L., Hobbs, D., & van Leeuwen, F. 2017, A&A, 603, A45

Charlot, P., et al. 2020, A&A, 644, A159

Fey, A. L., et al. 2015, AJ, 150, 58

Gödel, K. 1949, RvMoPh, 21, 447

Groenewegen, M. A. T. 2021, A&A, 654, A20

Korotky, V. A., Masár, E., & Obukhov, Y. N. 2020, Universe, 6, 14

Korotky, V. A., & Obukhov, Y. N. 1996, in Gravity Particles and Space-time, ed. P. Pronin, & G. Sardanashvily, 421 (arXiv gr-qc/9604049), doi: 10.1142/9789812830180_0021

Lindegren, et al. 2021, A&A, 649, A2

Lunz, S., Anderson, J. M., Xu, M. H., Titov, O., Heinkelmann, R., Johnson, M. C., & Schuh, H. 2023, A&A, 676, A11

Ma, C., et al. 1998, AJ, 116, 516

MacMillan, D. S., et al. 2019, A&A, 630, A93

Obukhov, Y. N. 1992, GReG, 24, 121

Petit, G., & Luzum, B. eds 2010, IERS Conventions 2010. IERS Technical Note No. 36

Schuh, H., & Behrend, D. 2012, J Geodyn, 61, 68

Soffel, M., Kopeikin, S., & Han, W.-B. 2017, JGeo, 91, 783

Titov, O., & Girdiuk, A. 2015, A&A, 574, A128

Titov, O., Lambert, S. B., & Gontier, A. M. 2011, A&A, 529, A91

Titov, O., Melnikov, A., & Lopez, Y. 2020, PASA, 37, e050

Titov, O., Krásná, H., Willcocks, S., Lopez, Y., & Osetrova, A. 2024, in 13th IVS General Meeting and 25th Anniversary, Tsukuba, Japan. Zenodo